

## The Turmoil in IC1262

Ginevra Trinchieri<sup>1</sup> and Corrado Saporiti<sup>2</sup>

<sup>1</sup> *INAF-Osservatorio Astronomico di Brera*

<sup>2</sup> *Università degli Studi di Milano*

IC1262, the brightest galaxy in a small group, is associated with extended X-ray emission, that breaks into a filamentary complex structure at the center. The new *Chandra* data clearly show that the morphology of the filaments is very peculiar on arcsec scale and that the structure is cooler than the surrounding medium and very sharply bounded. We found no clear association with the optical distribution of galaxies, indicating that the perturbation is peculiar to the hot phase of the IGM.

### 1. Why IC1262?

IC1262 is a bright early type galaxy classified as the cD of a poor group of galaxies (Wegner et al. 1999). First discovered in X-rays in the ROSAT All Sky Survey (RASS, Voges 1992; Voges et al. 1999), it was subsequently observed with the ROSAT HRI to investigate the nature of the high X-ray luminosity [ $L_x(0.2-2 \text{ keV}) \sim 4 \times 10^{43} \text{ erg/s}$ ] and X-ray-to-optical flux ratio. A complex structure on top of a very extended, more regular emission was immediately evident from the HRI data (Trinchieri & Pietsch 2000).

CHANDRA observations now reveal a spectacular morphology of the gas on arcsec/kpc scales (see Fig. 1) coupled to a temperature structure. This could indicate complex dynamics in the hot intergalactic medium (IGM), which is not seen at other wavelengths, suggesting once again that high quality X-ray observations are needed to characterize the ISM/IGM properties and to explore the full range of complexity that we are now finding more and more in groups and galaxies. In this presentation, we illustrate some of the preliminary results of the X-ray analysis of the *Chandra* data. *XMM-Newton* data will also be added to complete the picture. We assume a distance of 206 Mpc, which gives a scale of  $1' \sim 60 \text{ kpc}$ .

### 2. The New CHANDRA Data

Data obtained with ACIS-S in the imaging configuration (23 August 2001,  $\sim 31 \text{ ks}$ ) have been cleaned following the most recent threads provided by the <http://asc.harvard.edu/> site.

The raw image of the whole ACIS-S3 (CCD7) field is shown in Fig. 1 in the broad energy range 0.3–10 keV. Even in the raw data the complex structure at the center is evident, above a more diffuse extended component. The comparison between the X-ray and the optical images is shown in Fig. 3. Several point sources are seen in the field, often associated with optical objects.

#### 2.1. Morphology

The adaptively smoothed images (Fig. 2) enhance the morphology of the central  $\sim 5'$  region, and indicate that the structures are evident mostly in the band below  $\sim 2 \text{ keV}$ . An elongated arc-shaped enhancement in

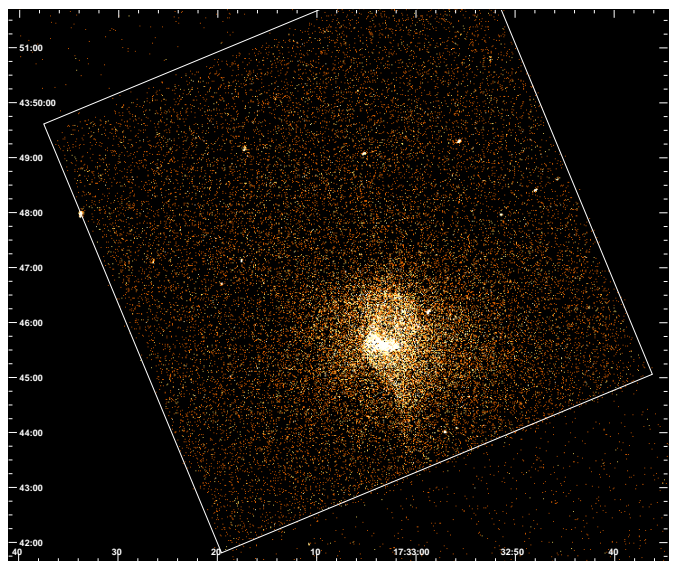


FIG. 1.— The raw image in the 0.3–10 keV energy band from CCD7. The white box illustrates the size and orientation of the CCD.

surface brightness, a central ellipsoid and a region of depressed emission just north of it are among the most notable features. A large scale emission, more regular and quite extended, is also detected in this source. At energies above 2.5 keV this is in fact the main component observed: it is flattened in the central region and shows a deviation toward the south reminiscent of the sharp feature seen at lower energies.

Since the source fills the entire CCD7 and goes beyond, to measure the total extent of the source we had to analyze adjacent CCDs, and we had to resort to the observations of blank field to estimate the background contribution. We normalized the background fields with the ratio of total counts in the 10–12 keV range (Markevitch et al. 2003 and <http://asc.harvard.edu>). This ratio is consistent with the ratio of the observing times, giving confidence to the level assumed for the background, and enabling us to use it also for the spectral analysis.

At radii larger than  $r \sim 2'$  the emission appears rather smooth, possibly slightly more extended and stronger in

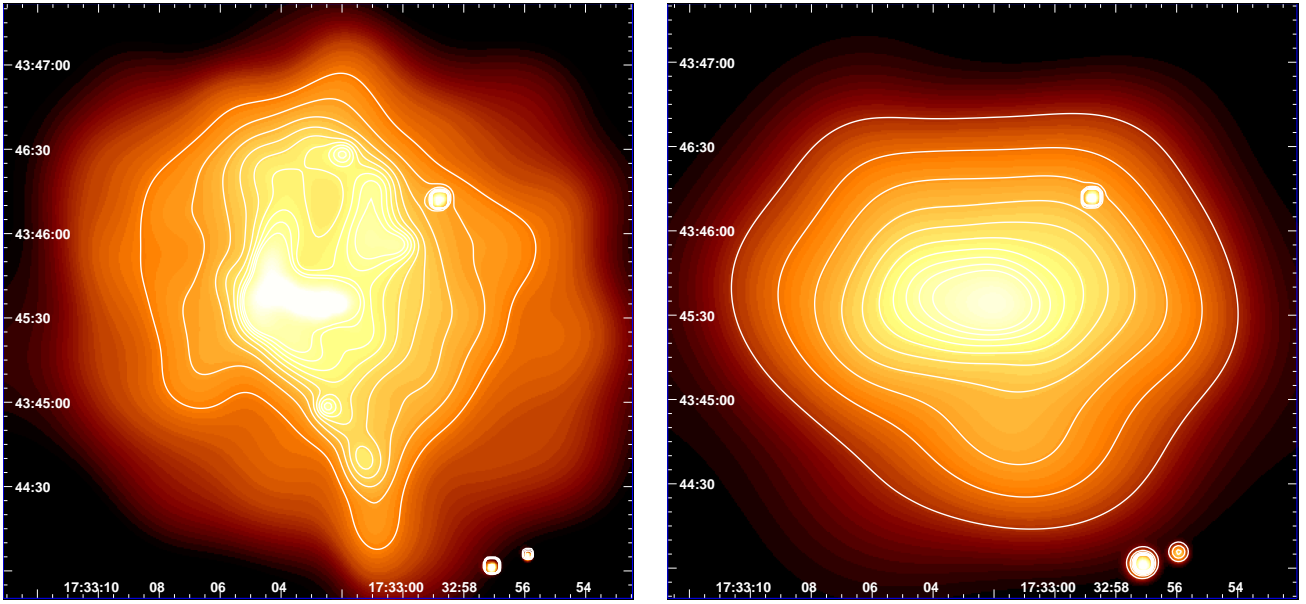


FIG. 2.— Adaptively smoothed images and X-ray contours of the central region of IC1262 in the 0.3–2.5 keV (LEFT) and 2.5–7 keV (RIGHT) energy ranges.

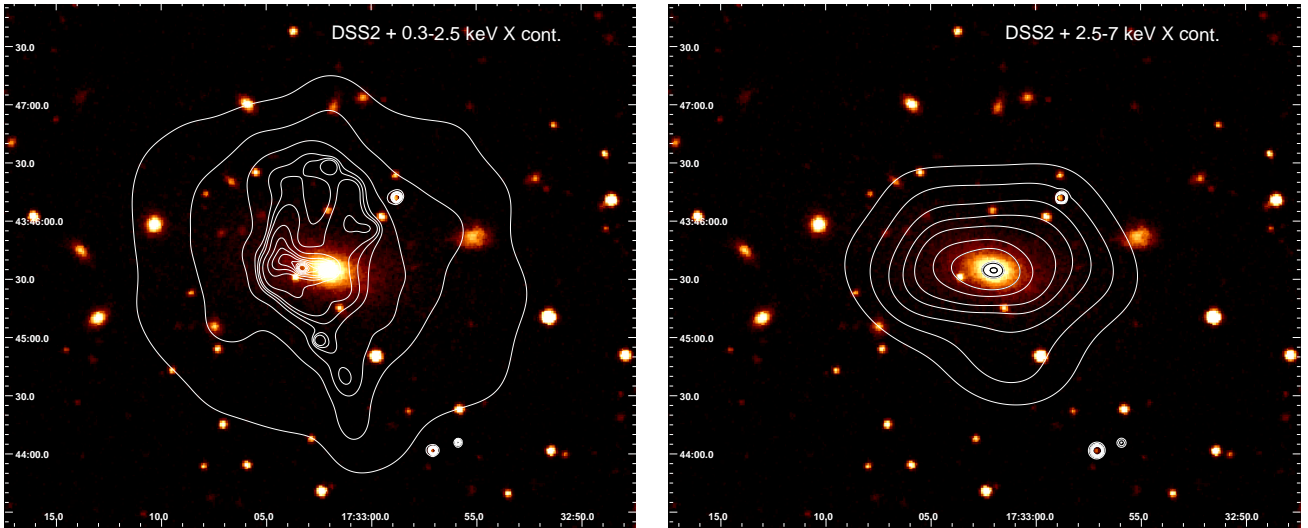


FIG. 3.— X-ray contours, from the maps of Fig. 2, are overlaid onto the optical image.

the southern direction (to be confirmed, since the data come from different CCDs). The radial profile in the 0.4–2.5 keV band, shown in Fig. 4, traces the emission to a distance of at least  $\sim 400\text{--}500''$ , corresponding to  $\sim 400\text{--}500$  kpc at the distance of the source. Outside these radii, the shape of the profiles become consistent with an almost constant level, which resembles closely the profile in the background fields. Such large extent indicates an association with the group around IC1262, rather than just with the galaxy itself. In the higher energy band, where the central structures are much weaker to non-existent, it is evident that the peak of the large scale emission (at  $\sim 17:33:01.8; +43:45:36$ ), is coincident with IC1262 (see also Fig. 3-right), supporting the classification of IC1262 as the central galaxy in the group.

Although generally peaked onto IC1262, the emission at the center of the large scale structure is clearly very complex, and even more striking if compared to the distribution of the optical objects in the region (Fig. 3-left): none of the structures resemble or coincide with galaxies or other optical counterparts. As already mentioned, some of the point-like sources (for example, to the NW and to the SW of IC1262, see Trinchieri & Pietsch 2000) coincide with optical counterparts, further indicating that the absolute coordinate system in the X-ray image is correct. It would appear that the perturbation is seen only in the distribution of the hot IGM.

As shown by the compressed isointensity levels in Fig. 2-left, we expect a steep gradient in the surface brightness distribution toward the E. In Fig. 5, radial

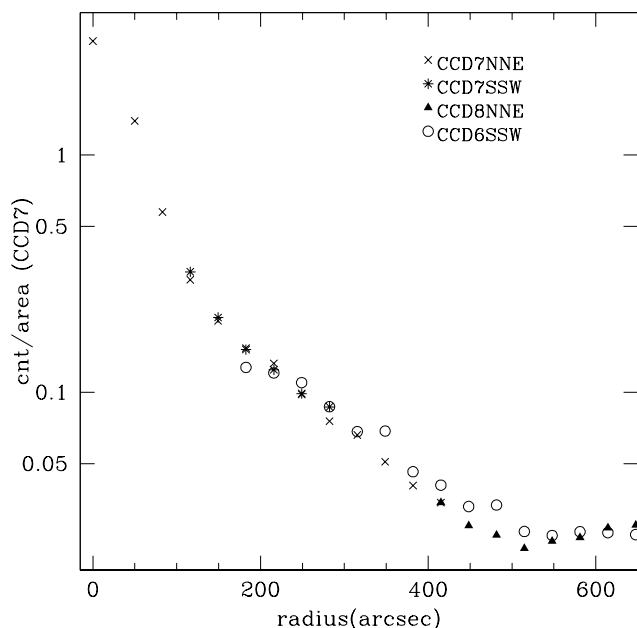


FIG. 4.— Radial profile of the emission in the energy range 0.4–2.5 keV. The emission is azimuthally averaged in concentric half annuli about the center (NNE and SSW directions, along the main axis of the CCDs). Data from CCD7 are used until available. At larger radii, the profile in the northern direction comes from CCD8, to the South we use the data from CCD6. Care was taken to mask out the regions outside the CCD boundaries. The vertical scale is the surface brightness (in counts/arcsec) measured from CCD7. The other data are normalized to the CCD7 level assuming azimuthal symmetry and imposing that the emission at a common radius (that per force comes from different angles of the same annulus) are the same.

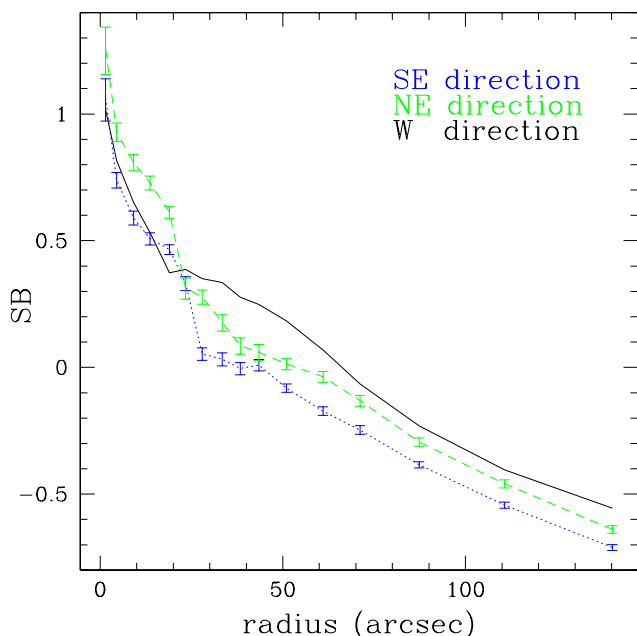


FIG. 5.— Radial profile of the central region in the 0.3–3 keV energy band. The emission is azimuthally averaged in angular sectors: the W half (solid line), the NE (dotted, blue) and SW (dashed, green) quadrants.

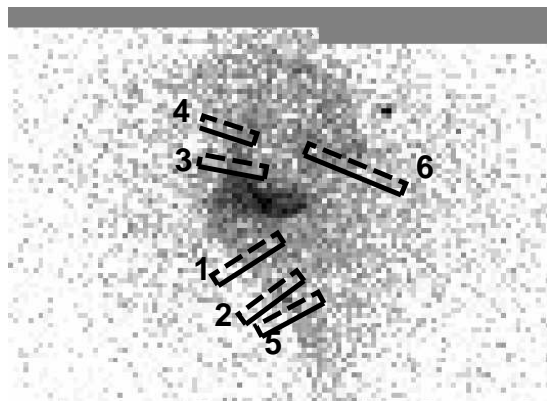


FIG. 6.— Locations of the regions of the “projections” in Fig. 7. Each box is  $5''$  thick, and is perpendicular to the sharp feature seen in the image.

profiles at the center are obtained in different angular sectors, the W half and the SE and NE quadrants. The surface brightness distributions to the E show larger and sharper jumps, but the profile is not smooth even in the W direction. Fig. 7 quantifies the amplitude of the “jumps” in surface brightness across the sharp edge of the arc-shaped feature in several different points (the regions used are plotted in Fig. 6). The projections shown in the figure indicate a factor of  $> 2\times$  surface brightness enhancement within one bin, of  $2''$  (corresponding to  $< 2$  kpc!!); this ratio is found to hold along the whole length of the structure ( $\sim 2.5$ ; 150 kpc). Region 2 also shows that the filament to the S is very narrow ( $\sim 2''$ ).

The other remarkable feature at the center appears to extend from IC1262 in the eastern direction in a shape of a “banana.” This feature also consists of a well defined, large enhancement in surface brightness (up to a factor of  $> 3$ ) although not as sharp as the Eastern feature. This structure becomes less compact toward the E, where it merges with the arc. Another sharp enhancement is seen to the NW (see Fig. 6 and Fig. 7), almost as a continuation of the “banana” to the NW that encloses a region of depressed emission.

## 2.2. Spectral Characteristics

The existence of a structure at the center of the large scale emission was already evident in the ROSAT data. Trinchieri & Pietsch (2000) suggested the presence of a shock that produced the structure. With the spectral information now available with *Chandra* it will be possible to better quantify the characteristics of the emission, in order to explain the origin of the central structure. We have already seen from the comparison of the different maps that the excess emission is seen mostly at lower energies, challenging already the idea of shocked IGM, that would require higher temperatures than the surrounding medium.

For the spectral analysis, we concentrate in the central region, where the peculiar structure is found. We have analyzed the area at radii greater than  $2'$ , in concentric annuli, with the main purpose of exploring possible radial variations of the spectral properties in the large scale

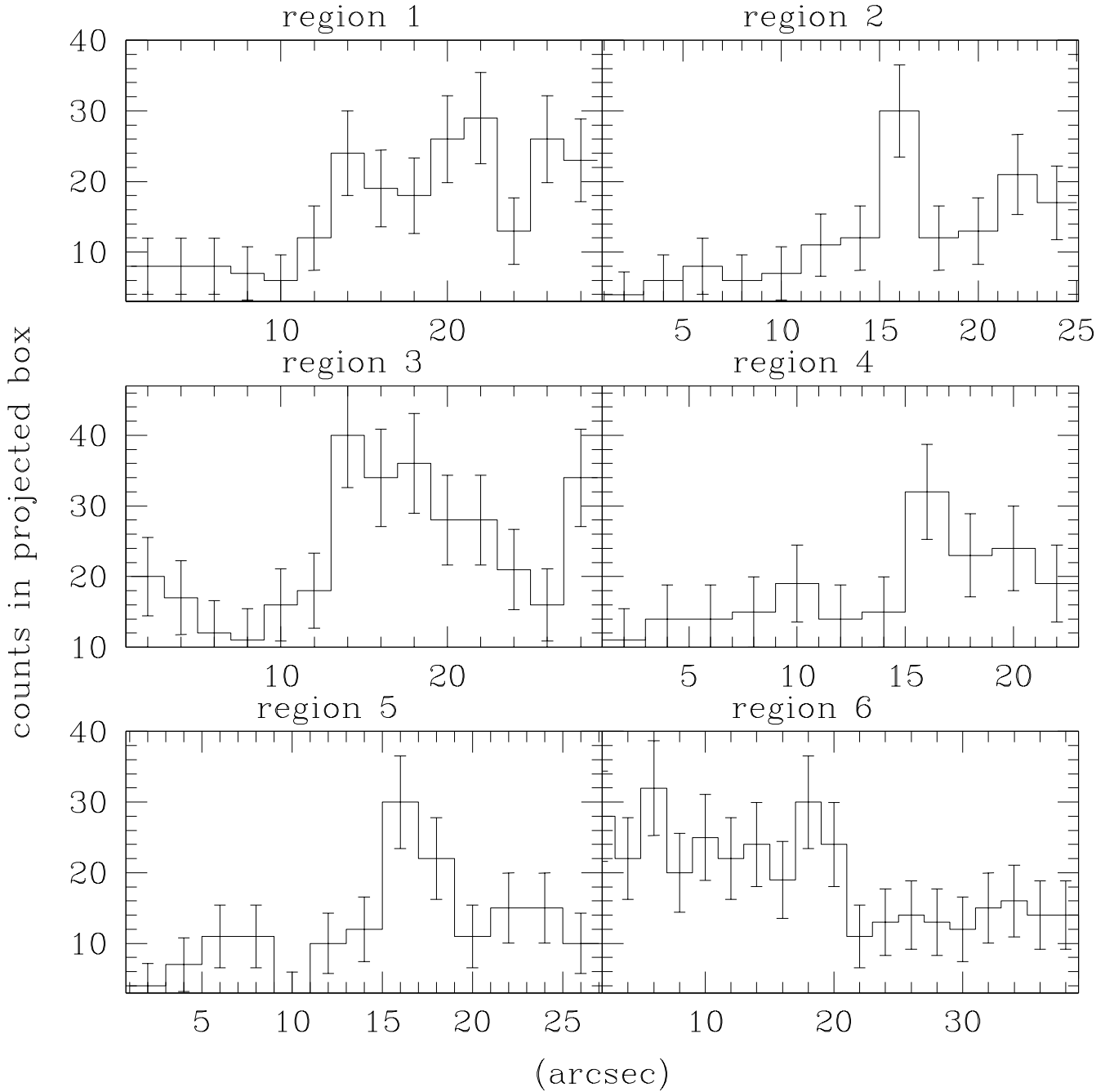


FIG. 7.— Example of projections across the E edge of the arc shaped feature (see Fig. 6). Each point (and statistical error) represents the counts in the 0.4–1.5 keV range in a box of  $\sim 2'' \times 5''$ . The surface brightness increases by at least factors of  $> 2$  within the space of 1 bin, or  $2''$ , corresponding to 2 kpc at the source distance.

IGM, and of determining an average spectrum to use as a comparison for the spectrum of the enhanced features, that could either be perturbations of the more extended structure, or totally unrelated features that we see projected onto it. We have used the CCD7 data only, and the blank fields as background. The data of all regions considered have been grouped to retain a significance of  $2.5\text{--}3\sigma$  in net counts. The outer regions have also been the subject of work by Hudson & Henriksen (2003) (see

also the presentations at this meeting).

As in other instances, we find that the model to represent the data is not unique. Here we limit ourselves to look for differences within a given model, and will consider elsewhere which is the most appropriate model for this region. In the example we show in Fig. 8 we have adopted a MEKAL code with abundances fixed at 0.3. With this model we can fit reasonably well an annulus at  $2'.5\text{--}3'$ , and the area of low surface brightness

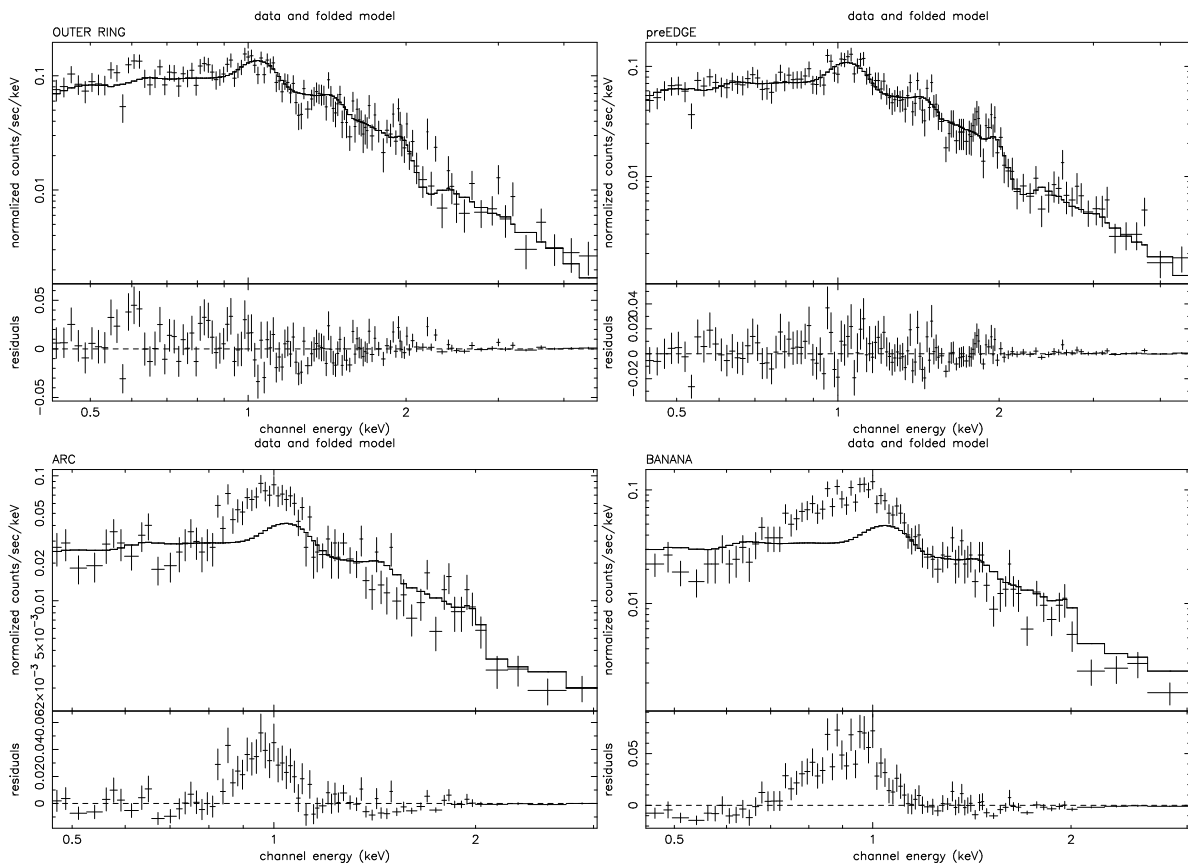


FIG. 8.— Top: Spectral data and residual for two regions, an annulus at  $\sim 2'5-3'$  and the low surface brightness region E of the arc, fitted by a single 2 keV temperature. Bottom: the same model is applied to the high surface brightness regions. In the “ARC,” the full length of the arc-shaped feature is considered. “Banana” consists of the central shape E of IC1262.

just E of the sharp arc edge (labeled “OUTER RING” and “preEDGE” respectively in the figure) with a temperature of  $\sim 2$  keV. The same model applied to either the “ARC” or the “BANANA” (bottom panels in Fig. 8) clearly fails to parameterize the data. A temperature of  $\sim 1$  keV instead provides a good fit to the data of both regions, confirming their softer nature relative to the surrounding lower surface brightness emission. Work is in progress to derive the spectral properties of different regions, to understand for example whether the same temperature applies to the whole high surface brightness emission in the center. The results will be used to derive physical parameters like density or cooling time more accurately than already done in Trinchieri & Pietsch (2000) [note that a temperature of 1 keV was assumed in that paper] to better understand the origin of these peculiar structures and their relation with the large scale IGM.

### 3. What Does This All Mean?

The large scale reservoir of hot IGM is regular in morphology and very well centered onto IC1262, as can be seen at energies above 2.5 keV, where the gas appears mostly unperturbed (although ellipsoidal in shape at the center). As discussed above, the perturbed structure

present at the center of this large scale emission has a significantly softer signature, and a very distinctive morphology, that might indicate a decoupling between the two structures.

The original interpretation of a shock front suggested by the ROSAT data (see Trinchieri & Pietsch 2000) can no longer simply apply, since the main feature of a shock, namely an increase in temperature at the density jump, is ruled out by the data.

Although at much cooler temperatures, the structure in IC1262 is reminiscent of cold fronts, sharp discontinuities in surface brightness coupled with lower gas temperatures embedded in a large scale hotter ambient medium, that have been recently observed in clusters of galaxies (Vikhlinin et al. 2001; Mazzotta et al. 2001; Markevitch et al. 2000). As in these other cases, a very sharp discontinuity is observed along the structures seen in this source, and the temperature in the high surface brightness regions is lower than at lower surface brightnesses.

Cold fronts are believed to form when a subcluster merges with a main structure and transport processes across the fronts are suppressed or greatly reduced (Ettori & Fabian 2000; Vikhlinin et al. 2001). While the X-ray evidence might suggest a similar phenomenon in IC1262, the peculiar morphology of the cold material is

so far rather unique. In most cases, cold fronts are identified as the sharp edges of relatively large and dense clouds. Filaments have also been observed in A3667 (Mazzotta et al. 2002), as a small perturbation compared to the bulk of the cold material, and are interpreted as hydrodynamical instabilities developing in the direction perpendicular to the motion. In IC1262 all of the cooler material is in a filamentary, distorted structure that would suggest a peculiar motion of the accreted material, if the cold filaments trace the path in the merging event. The large scale gas distribution also appears regular and reasonably azimuthally symmetric, suggesting that the perturbation is a local phenomenon in the center.

Moreover, unlike the cases of A3667, A2142 and A2034, that show evidences of merging or non equilibrium conditions in the optical data as well (Markevitch et al. 2000; Kempner et al. 2003; Vikhlinin et al. 2001) there is no reported evidence of disturbed morphologies in the optical or red images of IC1262 or of the group. However, Hudson & Henriksen (2003) find that a non-thermal component is required to fit the spectral data at radii 1.5–2.5 to the S and argue that this is indicative of a shock produced by the impact caused by a merger.

According to the optical classification, IC1262 is a cD

galaxy; the large scale distribution of the IGM would support this classification. At odds with it, and with the X-ray evidence, its velocity is lower than the systemic velocity given by Wegner et al. (1999) by almost 500 km s<sup>-1</sup>. However, before concluding that this discrepancy is real, a more complete assessment of the velocity field is required. So far, only a handful of redshifts have been measured in this region, and only for the brighter objects (mostly early types). Several fainter galaxies are visible in the vicinity of IC1262, but without knowing their distance it is not possible to associate them to the cD or the group.

Therefore the peculiar morphology at the center of IC1262 X-ray emission might be another example of cooler material acquired by the system and not yet mixed with the hotter ambient medium. Optical support to this interpretation is lacking at the present time, and a more thorough study at other wavelength, plus additional redshifts are necessary to complement the intriguing picture suggested by the X-ray data.

We acknowledge partial financial support from the Italian Space Agency (ASI).

### References

- Ettori, S., Fabian, A.C. 2000 MNRAS 317, L57  
 Hudson, D.S. & Henriksen, M.J. 2003, astro-ph 0308109  
 Kempner, J.C., Sarazin, C.L., Markevitch, M. 2003, astro-ph 0304310  
 Mazzotta, P. et al. 2001 ApJ555,205  
 Mazzotta, P., Fusco-Femiano, R., Vikhlinin, A. 2002, ApJ569, L34  
 Markevitch, M., Bautz, W., Biller, B. et al. 2003, ApJ583, 60  
 Markevitch, M., et al. 2000 ApJ541, 542  
 Trinchieri, G., & Pietsch, W. 2000, A&A 541, 487  
 Vikhlinin, A., Markevitch, M., Murray, S.s. 2001 ApJ551, 160  
 Voges, W. 1992, Proc.European IST Meeting Symposium, p9  
 Voges, W., Aschenbach, B, Boller, Th. et al. 1999 A&A 349 389  
 Wegner, G, Colless, M., Saglia, R., 199, MNRAS 305, 259